Published in "Nanoscale doi: 10.1039/C4NR00460D, 2014"
which should be cited to refer to this work.

Electronic Supplementary Information

In Vitro Dosimetry of Agglomerates

Vera Hirsch, Calum Kinnear, Laura Rodriguez-Lorenzo, Christophe A. Monnier, Barbara Rothen-Rutishauser, Sandor Balog and Alke Petri-Fink

Isothermal Titration Calorimetry (ITC)

From the known concentrations of tiopronin and Au-NPs ([Au] = 1 mM, corresponding to 14.7 nM of Au-NPs), the stoichiometry (N), affinity (K), and enthalpy changes (ΔH) upon binding were derived from an iterative fitting procedure to the data using a one-site binding model of the software Origin (Origin 8.5, OriginLab) provided with the MicroCal VP-ITC (Fig. S1 and Table S1). Taladriz-Blanco *et al.* reported similar values for the interaction between the thiol group of Penicillamine with citrate capped Au-NPs.[1] In an ITC study on the interactions of a 5'-thiol-labeled double-stranded DNA with a macroscopic Au surface, a binding equilibrium constant of $1.5 \pm 1.3 \times 10^6$ M^{-1} was found.[2] The higher degree of surface coverage compared to adsorbed Penicillamine found by Taladriz-Blanco *et al.* can be explained by the lower steric and electrostatic hindrance of close packing tiopronin molecules.[1,3]

Table S1. Thermodynamic parameters of the interaction of tiopronin with Au-NPs at 25°C

	Stoichiometry (N)	Surface coverage	K [M^{-1}]	ΔH [kcal·mol^{-1}]	ΔS [$J \cdot K^{-1} \cdot mol^{-1}$]
Tiopronin	1730 ± 9.0	67.4%	$(1.5 \pm 0.3) \times 10^7$	-26.1 ± 0.3	-54.7

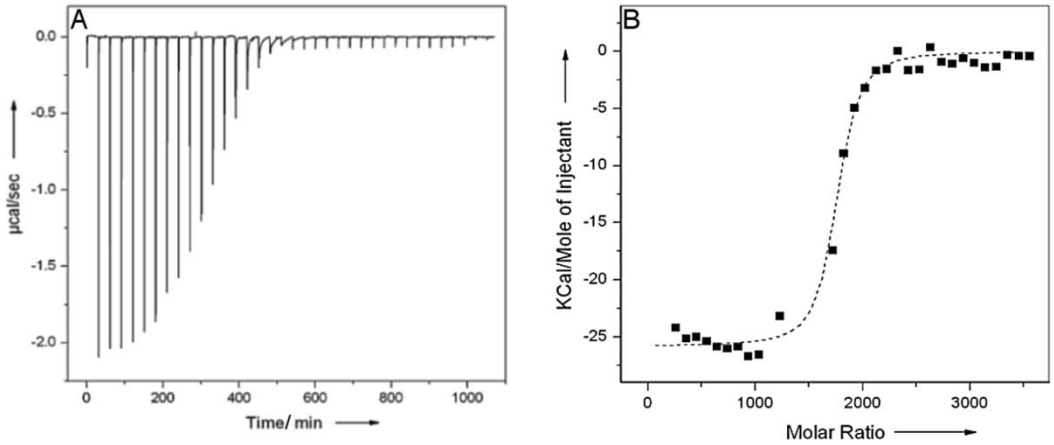

Fig.S1. ITC data for tiopronin (0.5 mM) with Au-NPs (14.7 nM). (A) Injections peaks (raw data vs. time) and (B) integrated injection peaks (kcal/mole of injectant vs. molar ratio) with iterative fit using a one-site binding model (dashed line) of the software Origin (Origin 8.5, OriginLab) provided with the MicroCal VP-ITC.

Agglomeration Kinetics

The aggregation process was induced by adding 1 M HCl solution to 2 mL of tiopronin coated Au-NP suspension, [Au] = 0.5 mM. The solution was homogenized by inversion and the self-assembly kinetics were recorded by UV-Vis.

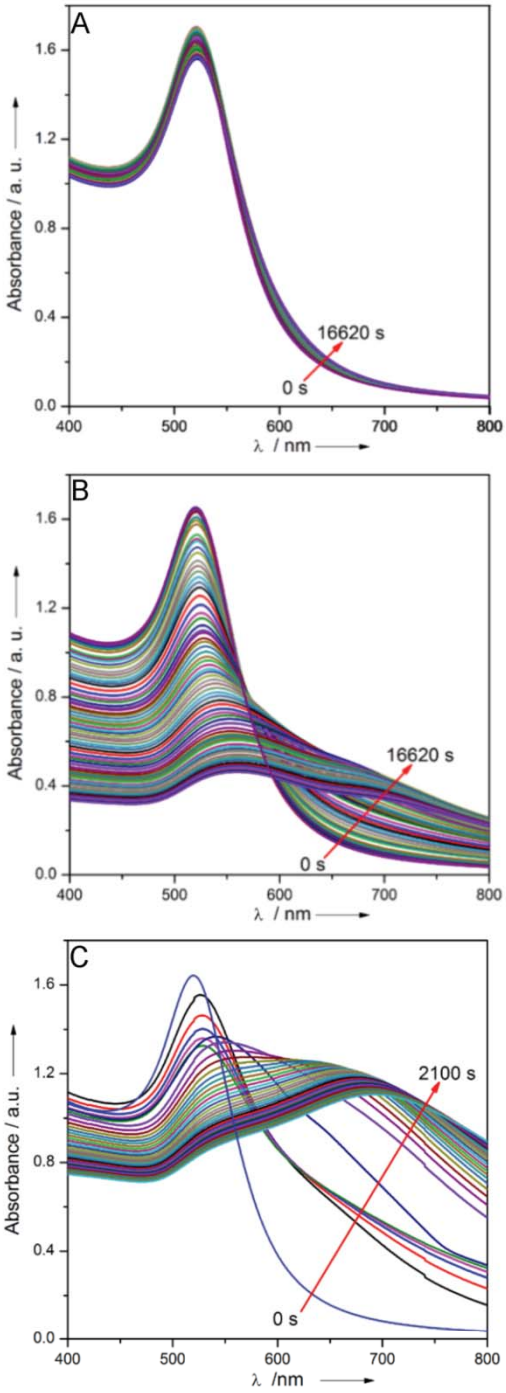

Fig.S2. Time evolution of the agglomeration process of Tio-Au-NPs at different pH: (A) 3.9; (B) 2.8; and (C) 2.6.

Complementary to this, time resolved dynamic light scattering (DLS) was undertaken with addition of different volumes of HCl (7.5, 10, or 15 µL HCl 1 M) to 2 mL of tiopronin coated Au-NP suspension, [Au] = 0.5 mM. Depolarized dynamic light scattering was not deemed necessary here due to the large agglomerates probed and their relatively slow rotational diffusion coefficients. The acid was placed on the underside of the sample vial cap, before rapidly mixing twice by inversion and immediately starting measurements. Scatter was collected at 90° for duration of 20 seconds over 50 minutes. The hydrodynamic radius was calculated via the 2nd order cumulants for every 20 second measurement, and plotted as a function of time or the natural logarithm of time. The average mass of agglomerates formed from the process of diffusion limited cluster aggregation (DLCA) increases linearly with time, which means that the radius scales as $R \propto t^{1/d_f}$ whereas if the process is reaction limited cluster aggregation (RLCA) then the radius scales as $R \propto e^{Ct}$ where d_f is the fractal dimension and C is an experiment dependent constant.[4-6] Therefore, a plot of $\ln(R)$ against $\ln(t)$ should be linear for RLCA behavior, while a plot of $\ln(R)$ against t should be linear for DLCA behavior. The time resolved DLS indeed shows typical RLCA behavior at high pH (7.5 µL HCl) and typical DLCA behavior at low pH (15 µL HCl) (Figure S3). This is consistent with the UV-Vis characterization (Figure S2).

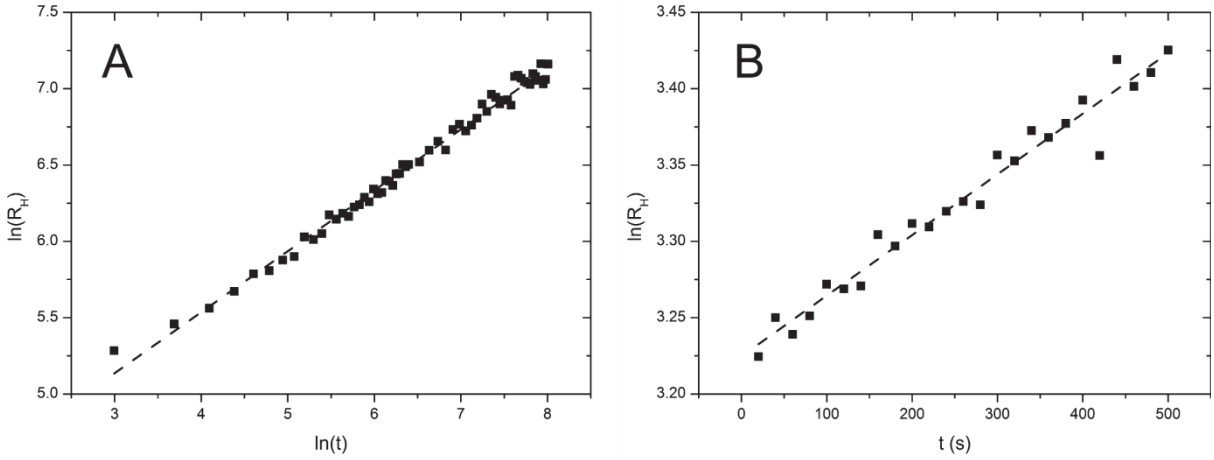

Fig.S3. Time evolution of the hydrodynamic radius for the agglomeration process of Tio-Au-NPs at different volumes of HCl: (A) 7.5 µL; (B) 15 µL.

Colloidal Stability

UV-Vis spectra of the single PVA coated Tio-Au-NPs (single Au-NPs) and the prepared agglomerates (agglomerates-1 or agglomerates-2) were recorded using a Jasco V-670 spectrophotometer. The samples were diluted 1 fold in water, PBS or cell culture medium (Fig. S4). The UV-Vis spectra of the PVA coated single Au-NPs at different pH values shows a clear red shift of the localized surface plasmon resonance (LSPR) band as the NPs agglomerate.[7] After dilution in PBS and Cell culture Medium the UV-Vis spectra show comparable LSPR bands, indicating the stability of the polymer coated NPs and agglomerates at physiological pH.

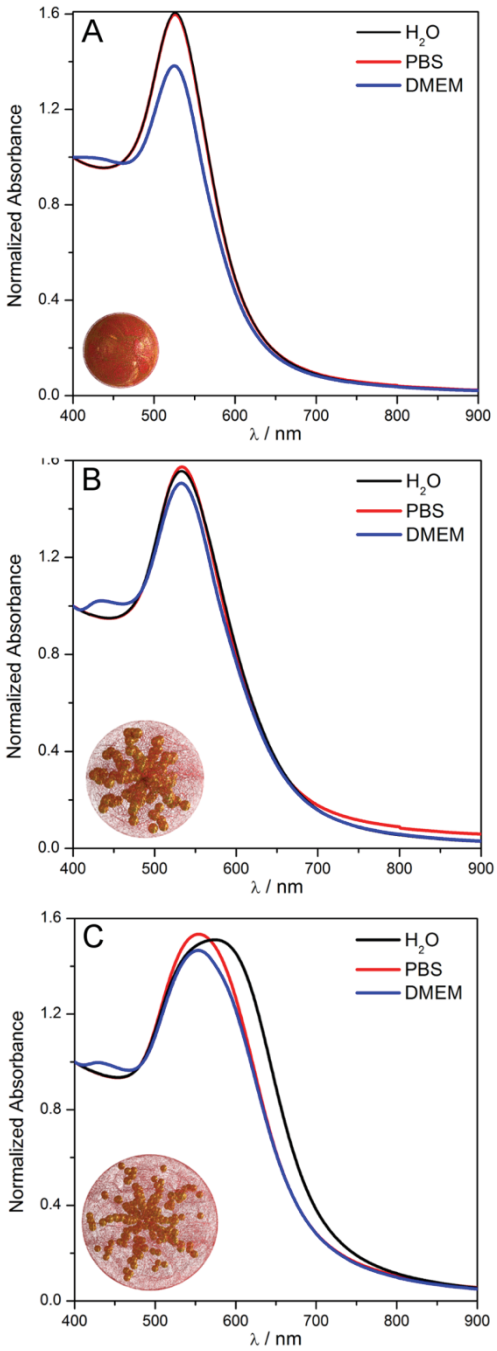

Fig.S4. UV-Vis spectra of (A) single Au-NPs, (B) Au agglomerates-1, and (C) Au agglomerates-2 kept in water, PBS buffer and DMEM medium. The particles were incubated in PBS and DMEM for 24 h. The spectra were normalized based on their absorbance at 400 nm.

Depolarized Dynamic Light Scattering (DDLS)

Coherent laser light becomes partially depolarized upon scattering from gold NPs, and depolarization provides a tool to probe rotational diffusion. For uniform particles, the temporal correlation function follows a negative exponential: $g1_{vh}(t) = e^{-Y t}$ and the equivalent hydrodynamic radius, R_H, is calculated via $Y = q^2 \frac{k_B T}{6 \eth h R_H} + \frac{3 k_B T}{4 \eth h R_H{}^3}$, where k_B is the Boltzmann constant, T is the temperature, h is the viscosity of water, and q is the scattering vector modulus $q = \frac{4\eth}{\grave{e}} n \sin\left(\frac{\grave{e}}{2}\right)$ and n is the refractive index of water.

The Schulz-Zimm distribution (Eq. S1) was applied to describe polydispersity, and is characterized by two parameters: m is the mean, and p relates to the polydispersity index (SD/mean = $1/\sqrt{1+p}$). G(x) is the Gamma function.

$$p_Y(m,p,Y) = \frac{e^{-\frac{(1+p)Y}{m}}\left(\frac{1+p}{m}\right)^{1+p} Y^p}{G(1+p)} \quad \text{(S1)}$$

The Laplace transform of the Shulz-Zimm distribution provides the correlation function (Eq. S2) we used for interpreting the scattering results (Fig.S5).

$$g1_{vh}(m,p,t) = \left(\frac{1+p}{1+p+m\,t}\right)^{1+p} \quad \text{(S2)}$$

and the intensity weighted hydrodynamic radius was obtained via Eq. S3:

$$m = q^2 \frac{k_B T}{6\,\eth\, h\, R_H} + \frac{3\,k_B T}{4\,\eth\, h\, {R_H}^3} \quad \text{(S3)}$$

The use of this distribution allowed a good fit to the measured correlation function, thereby providing a more accurate measure of the mean hydrodynamic radius compared to the more common cumulant analysis, which is only valid at low polydispersity.[8] For all subsequent calculations with the ISDD model, the mean hydrodynamic radius was used.

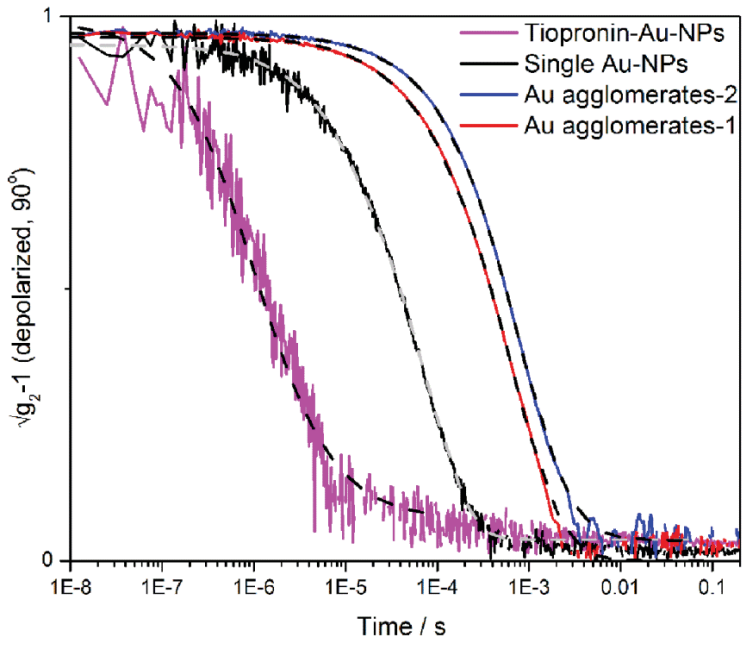

Fig.S5. Temporal correlation functions recorded for single Au-NPs and corresponding agglomerates (solid line). The dashed lines are the best fits of Eq. S2.

Calculation of diffusion and sedimentation parameters

The hydrodynamic size of the NPs and the agglomerates was measured by DDLS (Table 1 in the report) and the number of particles per aggregate was counted from cryo-TEM images (Table S2). The estimated density of PVA in water is negligible compared to that of water; therefore the density of the remaining volume was set to 1 g/cm^3.

The sedimentation velocity can be calculated from *Stokes' law* (Eq. S4), where g is the gravitational acceleration, and ñ and $\tilde{n}_m$ are the mass densities of the NP (or agglomerates) and the medium, respectively.[9]

$$V_S = \frac{2g}{9\mu} \cdot (\tilde{n} - \tilde{n}_m) \cdot r^2 \quad \text{(S4)}$$

An effective velocity of diffusion was calculated using equation (Eq. S5, Reference 6), where the variable *t* (time) was substituted from the *Einstein equation*: $\langle \Delta x^2 \rangle = 2 \cdot D \cdot \Delta t$. The diffusion coefficient, *D*, was calculated from the measured size by DDLS.

$$V_D = \left(\frac{x}{t}\right) = \frac{2D}{x} \quad \text{(S5)}$$

This result for the velocity of diffusion is only characteristic over a specific length, or time, which was chosen in reference7 to be set to x=1 mm. In order to compare our findings to the conclusions drawn *a posteriori* by Cho *et al.* we also set x=1 mm (Table S3).[10]

Table S2. Number of particles counted per agglomerate from cryo-TEM images

agglomerates-1	Number of particles counted per agglomerate	Average	SD
1	10		
2	9		
3	9		
4	9	8.86	0.90
5	7		
6	9		
7	9		
agglomerates-2	**Number of particles counted per agglomerate**	**Average**	**SD**
1	34		
2	36		
3	42		
4	29		
5	37	33.78	5.33
6	31		
7	38		
8	24		
9	33		

Table S3. Calculated diffusion and sedimentation parameters

Parameter	Tio-Au-NPs	single Au-NPs	agglomerates-1	agglomerates-2
Particle Diameter / nm	19	65	145	168
Diffusion Coefficient (D)/ $m^2 s^{-1}$	3.64E-11	9.94E-12	4.56E-12	3.90E-12
Diffusion Velocity (V_D)/ $m s^{-1}$	7.28E-08	1.99E-08	9.11E-09	7.80E-09
Number particles per agglomerate	1	1	8.86	33.78

Volume gold/ cm^3	1.53E-18	1.53E-18	1.36E-17	5.17E-17
Mass of gold/ g	2.96E-17	2.96E-17	2.62E-16	9.98E-16
Volume of NP or agglomerate/ cm^3	3.06E-18	1.51E-16	1.56E-15	2.48E-15
Remaining volume/ cm^3	1.53E-18	1.49E-16	1.55E-15	2.43E-15
Remaining mass /g	1.53E-18	1.49E-16	1.55E-15	2.43E-15
Total mass/ g	3.11E-17	1.79E-16	1.81E-15	3.43E-15
Effective density/ g/cm3	10.18	1.19	1.16	1.38
Effective density/ kg/m3	1.02E+4	1.19E+3	1.16E+3	1.38E+3
Sedimentation Velocity (V_S)/ m s^{-1}	2.33E-09	6.60E-10	2.70E-09	8.60E-09
V_S/V_D	0.032	0.03	0.30	1.10
V_D *1E-8 m s^{-1}	7.28	1.99	0.91	0.78
V_S *1E-8 m s^{-1}	0.93	0.26	1.08	3.44

Relative Cellular Uptake

The ISDD model provided by Hinderliter *et al.* was used to estimate the cellular dose as function of time, for the three particle types.[11] In a dilute and quiescent NP suspension where collective fluid motion, turbulence, and inter-particle interactions are absent, the displacement of NPs is governed by sedimentation and diffusion. With these conditions, the equation of motion of monodisperse NPs can be described in terms of concentration as a function of depth (x) and time (t):[12]

$$\frac{\partial n(x,t)}{\partial t} = D\frac{\partial^2 n(x,t)}{\partial x^2} - V\frac{\partial n(x,t)}{\partial x} \quad \text{(S6)}$$

D and V are the diffusion coefficient and settling velocity of the NPs, respectively, given by Stokes' law and the Stokes-Einstein equation:

$$D = \frac{k_B T}{6\,\eth\, h\, R_H} \quad \text{(S7)}$$

$$V = \frac{2g}{9\,h} \cdot (\tilde{n} - \tilde{n}_m) \cdot R_H^2 \quad \text{(S8)}$$

where R_H is the Stokes radius, k_B is the Boltzmann constant, T is the temperature, h is the dynamic viscosity of the fluid, g is the gravitational acceleration constant, and p and p_m are the mass densities of the NPs and the fluid.[9,13] To estimate the time-dependent cellular dose from NPs, Hinderliter *et al.* adapted Eq. S6, postulating that from the point of view of cellular dose only the vertical movement is relevant while the lateral movement of the particles is not. Eq. S6 has been solved with the following initial and boundary conditions: at the beginning of the experiment the NPs are homogenously distributed in the fluid, and as soon as a NP contacts the cell surface it becomes internalized instantly by the cell and remains within the cell. The input variables used for

each particle type was the average hydrodynamic radius, obtained from DDLS, and the effective density of the NP or agglomerate, which was described in the previous section on sedimentation and diffusion velocity calculations. With the initial and boundary conditions, and the input variable described above, Equation S6 was solved using the partial differential equation solver in Matlab® (Mathworks, Inc.) giving the number of particles present at the bottom of the well as a function of time. This was compared with the experimentally measured cellular dose (Figure S6)

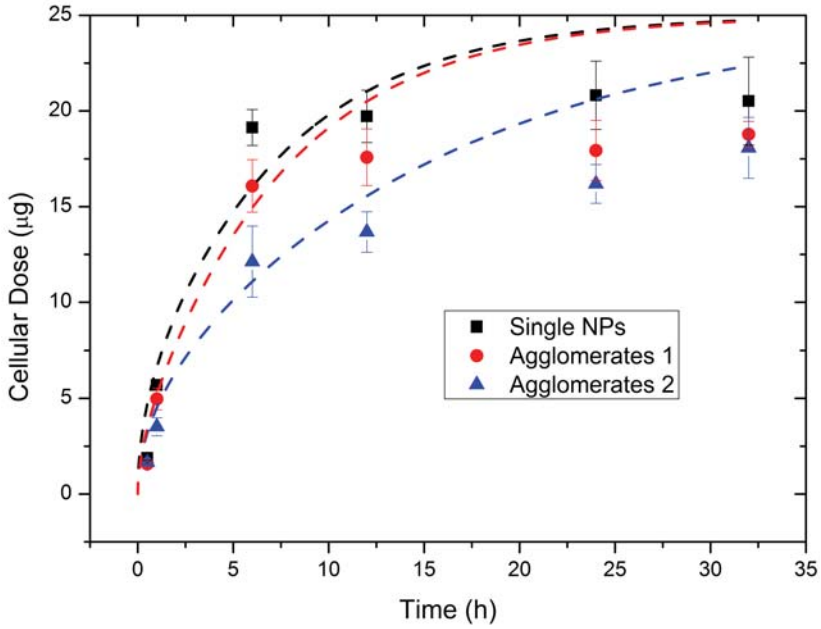

Fig. S6. NP uptake as function of time as measured by ICP-OES (n = 5; Error Bar = SD). Dashed line: ISDD model.

The model assumes, however, ideal conditions and does not account for, among others, collective motions of the media influenced through pipetting of the particle suspensions into the cell culture. Therefore a time dependent but otherwise unknown factor which accounts for these effects, was defined as *a(t)* and was assumed to be equal for each cell uptake experiment. The cell uptake of *e.g.* the single NPs can then be estimated from $f_X(t)*a(t)$. In contrast to the absolute values of cellular dose, $f_x(t)*a(t)$, the relative cell uptake between two particle types allows the elimination of the time dependent factor *a(t)*. (Ex. S1). The results of this ratiometric approach are given in Figure 4.

$$\frac{f(t)_{\text{single Au-NPs}} * \mathbf{a(t)}}{f(t)_{\text{agglomerates-1}}(t) * \mathbf{a(t)}} = \frac{f(t)_{\text{single Au-NPs}}}{f(t)_{\text{agglomerates-1}}(t)} \qquad \text{(Ex. S1)}$$

Cytotoxicity

Fig. S7 shows the release of Lactate Dehydrogenase (LDH) by HeLa cells relative to the positive control, Triton X-100, after 24h exposure.

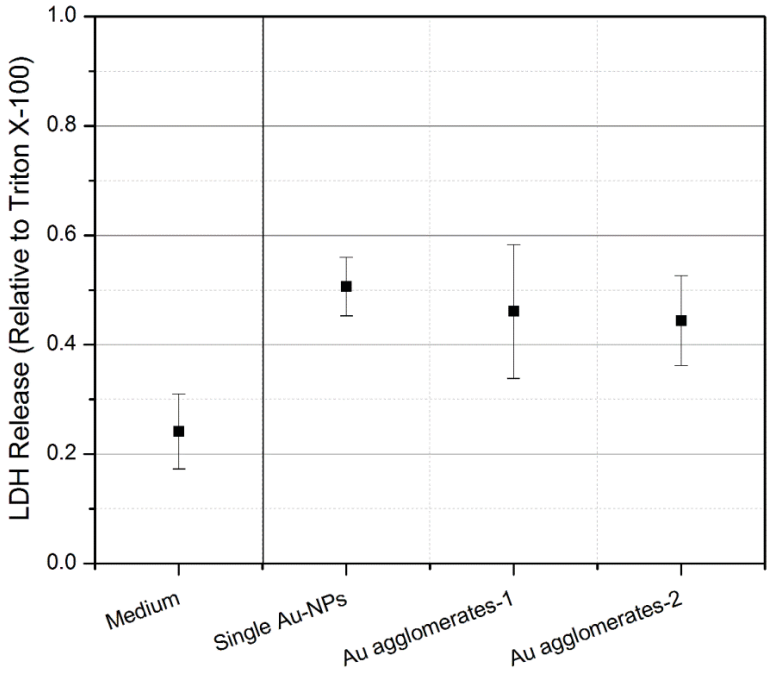

Fig.S7. Release for lactate dehydrogenase (LDH) from HeLa cells relative to Triton X-100 after 24h suspension exposure to single Au-NPs, as well as Au agglomerates 1 and 2 (n=5, Error Bars= SD). A pairwise t-test was performed and significance was indicated by: *p <0.05 versus medium.

Control – large spherical gold nanoparticle

The large spherical Au-NPs were synthesized by overgrowth of gold onto the citrate-capped Au-NPs from earlier, before functionalization with tiopronin. The first growth step was carried out by the addition of hydroxylamine-hydrochloride ($NH_2OH{\cdot}HCl$; 1.96 mM) a solution of gold salt ($HAuCl_4.3H_2O$; 0.25 mM) followed by addition of the seed suspension (citrate-Au-NPs; 2.26 x 10^{-5} M) resulting in spherical NPs of approximately 60 nm in diameter. A second growth step was made following the same procedure as the first step with adjusted concentrations: 0.5 mM of $HAuCl_4.3H_2O$, 2.78 mM of $NH_2OH{\cdot}HCl$, and 4.6 x 10^{-6} M of 60nm-diameter Au-NPs. This resulted in NPs with a diameter of 135 nm which were subsequently functionalized with PVA (7 mL of the same concentration as used for the stabilization of the aggregates) and washed by centrifugation at 350 ×g for 25 mins, and redispersed in PBS.

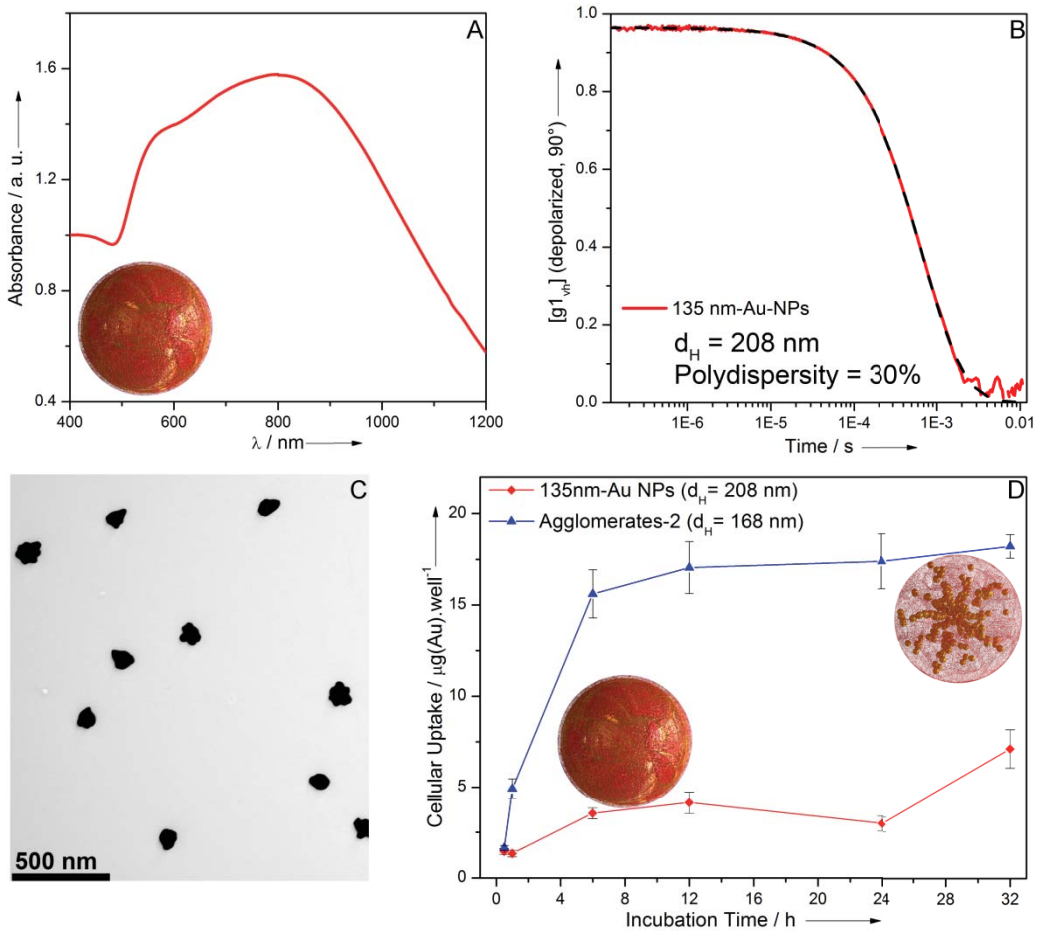

Fig.S8. (A) UV-Vis spectrum, (B) temporal correlation function (the dashed lines are the best fit of Eq. S2) and (C) TEM image of PVA-coated Au-NPs with a core of d = 135 ± 18 nm. (D) Quantification of intracellular Au by ICP-OES as a function of incubation time (n = 5, Error Bars = SD). Cell uptake of these solid particles was compared with the obtained for agglomerates-2 sample.

References

1 P. Taladriz-Blanco, N. J. Buurma, L. Rodríguez-Lorenzo, J. Pérez-Juste, L. M. Liz-Marzán and P. Hervés, *J. Mater. Chem.* 2011, **21**, 16880.
2 M. Yang, H. C. M. Yau and H. L. Chan, *Langmuir*, 1998, **14**, 6121–6129.
3 A. C. Templeton, S. Chen, S. M. Gross and R. W. Murray, *Langmuir*, 1999, **15**, 66–76.
4 M. Y. Lin, H. M. Lindsay, D. A. Weitz, R. Klein, R. C. Ball and P. Meakin, *J. Phys.: Condens. Matter*, 1990, **2**, 3093–3113.
5 M. Lin, H. Lindsay, D. Weitz, R. Ball, R. Klein and P. Meakin, *Phys. Rev. A*, 1990, **41**, 2005–2020.
6 R. Ball, D. Weitz, T. Witten and F. Leyvraz, *Phys. Rev. Lett.* 1987, **58**, 274–277.
7 T. Ung, L. M. Liz-Marzán and P. Mulvaney, *J. Phys. Chem. B*, 2001, **105**, 3441–3452.
8 S. Balog, L. Rodriguez-Lorenzo, C. A. Monnier, B. Michen, M. Obiols-Rabasa, L. Casal-Dujat, B. Rothen-Rutishauser, P. Schurtenberger and A. Petri-Fink, *In Preparation*.
9 Crank J. *The Mathematics of Diffusion*, Oxford University Press, Oxford, England, 2nd edn. 1975.
10 E. C. Cho, Q. Zhang and Y. Xia, *Nat. Nanotech.* 2011, **6**, 385–391.
11 P. M. Hinderliter, K. R. Minard, G. Orr, W. B. Chrisler, B. D. Thrall, J. G. Pounds and J. G. Teeguarden, *Part. Fibre Toxicol.* 2010, **7**, 36.
12 M. Mason and W. Weaver, *Phys. Rev.* 1924, **23**, 412–426.
13 A. Einstein, *Ann. Phys.* 1905, **322**, 549–560.